Transfer function analysis of the circulation: unique insights into cardiovascular regulation

J. PHILIP SAUL, RONALD D. BERGER, PAUL ALBRECHT,
STEPHEN P. STEIN, MING HUI CHEN, AND RICHARD J. COHEN
*Harvard-Massachusetts Institute of Technology Division of Health Sciences and Technology,
Cambridge 02139; Department of Cardiology, Children's Hospital, Department of Medicine,
Brigham and Women's Hospital, and Departments of Pediatrics and Medicine,
Harvard Medical School, Boston, Massachusetts 02115*

SAUL, J. PHILIP, RONALD D. BERGER, PAUL ALBRECHT, STEPHEN P. STEIN, MING HUI CHEN, AND RICHARD J. COHEN. *Transfer function analysis of the circulation: unique insights into cardiovascular regulation.* Am. J. Physiol. 261 (Heart Circ. Physiol. 30): H1231-1245, 1991.—We have demonstrated previously that transfer function analysis can be used to precisely characterize the respiratory sinus arrhythmia (RSA) in normal humans. To further investigate the role of the autonomic nervous system in RSA and to understand the complex links between respiratory activity and arterial pressure, we determined the transfer functions between respiration, heart rate (HR), and phasic, systolic, diastolic, and pulse arterial pressures in 14 healthy subjects during 6-min periods in which the respiratory rate was controlled in a predetermined but erratic fashion. Pharmacological autonomic blockade with atropine, propranolol, and both, in combination with changes in posture, was used to characterize the sympathetic and vagal contributions to these relationships, as well as to dissect the direct mechanical links between respiration and arterial pressure from the effects of the RSA on arterial pressure. We found that *1)* the pure sympathetic (standing + atropine) HR response is characterized by markedly reduced magnitude at frequencies >0.1 Hz and a phase delay, whereas pure vagal (supine + propranolol) modulation of HR is characterized by higher magnitude at all frequencies and no phase delay; *2)* both the mechanical links between respiration and arterial pressure and the RSA contribute significantly to the effects of respiration on arterial pressure; *3)* the RSA contribution to arterial pressure fluctuations is significant for vagal but not for sympathetic modulation of HR; *4)* the mechanical effects of respiration on arterial pressure are related to the negative rate of change of instantaneous lung volume; *5)* the mechanical effects have a higher magnitude during systole than during diastole; and *6)* the mechanical effects are larger in the standing than the supine position. Most of these findings can be explained by a simple model of circulatory control based on previously published experimental transfer functions from our laboratory.

spectral analysis; respiratory arrhythmia; autonomic nervous system

---

RESPIRATORY ACTIVITY continually perturbs cardiovascular hemodynamics through a number of direct and indirect mechanisms. In the brain stem, respiration modulates the activity of most sympathetic and vagal efferents both through direct coupling between the respiratory and autonomic centers and through modulation of central sensitivity to baroreceptor and other afferent inputs (4, 20, 31, 34). The autonomic efferents in turn modulate heart rate (HR) and peripheral vascular resistance with respiratory periodicities. In addition, when phrenic nerve signals are transmitted into mechanical ventilation, respiration directly and indirectly influences arterial and central venous pressures and flows through mechanical thoracic coupling and changes in left and right ventricular preload (6, 7). Finally, changes in arterial P_{CO_2}, P_{O_2}, and pH, which result from short- and long-term changes in respiratory activity, modulate the activity of both afferent and efferent autonomic nerves in the brain stem and the periphery and the central sensitivity to afferent impulses (23). These complex and constant effects of respiration on virtually every aspect of the cardiovascular system have intrigued physiologists, engineers, and clinicians for centuries and make respiration a unique probe for studying cardiovascular control.

The one limitation to this respiratory probe from a systems analysis standpoint is that in resting animals and humans the respiratory rate is relatively fixed, thereby limiting the frequency content of the perturbing signal and of the responses obtained. However, we have demonstrated previously that the frequency content of the respiratory signal can be effectively broadened by having subjects voluntarily breathe with random intervals predetermined by a series of auditory cues (12). Furthermore, we showed that this broadened respiratory signal can be used to efficiently identify the magnitude and phase of the transfer function (or frequency response) between respiration and HR in a similar fashion to the way an engineer might characterize an audio speaker, a cardiologist a hemodynamic catheter, or an audiologist the human ear. We found that the broadband transfer function accurately reproduces the data obtained from breathing at multiple individual frequencies (fixed rates) and has characteristics that change significantly with the relatively mild perturbation of a change in posture (40). In this study, we sought to use this technique to precisely define the sympathetic and vagal contributions to the respiratory sinus arrhythmia

(RSA), and to investigate the complex links between respiration and arterial blood pressure.

METHODS

Subjects. Fourteen male nonsmoking adult volunteers (ages 19–38 yr, median 21 yr) participated in the study. No subject had a history of cardiopulmonary disease. Subjects did not consume caffeinated beverages on the day of the study. All experiments were performed between 10 A.M. and 4 P.M. and 2–4 h after the last meal. The experimental protocol was fully approved by the Massachusetts Institute of Technology Committee on the Use of Humans as Experimental Subjects, and written informed consent was obtained before each procedure. All experiments were performed in the Clinical Research Center at the Massachusetts Institute of Technology.

Measurements. One lead of the surface electrocardiogram (ECG), changes in the instantaneous lung volume (ILV), and radial artery pressure were recorded on an eight-channel FM tape recorder (Hewlett-Packard 3968A). Lung volume changes were measured with a two-belt chest-abdomen inductance plethysmograph (Respitrace Systems). Arterial pressure was measured with a 22-gauge Teflon catheter in the radial artery of the nondominant hand. A 3-ml/h infusion of heparinized saline (2 U/ml) was maintained through the catheter. An intravenous line was also placed for administering normal saline and pharmacological agents. Data were collected in six 13-min segments. Before each period of data collection, a respiratory calibration signal was recorded by having the subject alternately empty and fill an 800-ml bag.

Respiratory control. Subjects were instructed to initiate a breath with each tone of a series of auditory cues. The sequence of tones was generated by a computer and recorded on cassette tape for playback during each experiment. The computer was programmed to initially space the tones evenly in time at a preset rate of 12 breaths/min to allow the subject to find a comfortable depth of inspiration. The program then switched to a mode in which the tones were spaced at irregular intervals, but with the same mean rate of 12 breaths/min. The respiratory intervals in the latter mode were chosen according to a modified Poisson process because the power density of a sequence of Poisson impulses is constant over all frequencies. Thus the power spectrum of the respiratory drive chain was nearly flat (without preferred peaks), and the frequency content of the measured lung volume signal was effectively whitened. Minimum and maximum intervals of 1 and 15 s were chosen to avoid discomfort. Although the respiratory intervals were controlled, the subjects were allowed to comfortably control the depth and shape of each breath throughout the experiment to preserve normal ventilation. To help subjects anticipate the appropriate size breath, the length of each trigger tone varied between 50 and 400 ms in direct proportion to the duration of the upcoming interval. A complete discussion of the rationale behind and details of the chosen interval sequence has been described by Berger et al. (12).

Experimental protocol. After instrumentation, each subject was asked to practice breathing to the irregular sequence of tones for 1–2 min. With the subject supine, a calibration signal was then recorded using the 800-ml bag. The subject was asked to breathe to the recorded tone sequence beginning with the fixed rate intervals and followed by 13 min of irregular intervals. The subject was moved to the standing position, and after a minimum of 5 min for hemodynamic equilibration, the calibration procedure and breathing protocol were repeated. We will refer to these conditions, before any autonomic blockade, as the supine and standing control states. The subject was then returned to the supine position and given either atropine (0.03 mg/kg, $n = 7$) or propranolol (0.2 mg/kg, $n = 7$). After 10 min for equilibration, the above breathing protocol was repeated with the subject supine and standing. The subject was again returned to the supine position and given the other autonomic blocking agent. The supine and standing breathing protocols were repeated under double blockade for all 14 subjects.

The doses chosen for complete parasympathetic blockade (atropine) and complete β-adrenergic blockade (propranolol) were based on previous studies (25). Because HR control is primarily via the vagus in normal supine humans, the above protocol allowed for an investigation of pure parasympathetic modulation of HR when subjects were in the supine position after propranolol. Because sympathetic outflow increases from very low levels when the position is changed from supine to standing, pure sympathetic modulation could be investigated when subjects were in the standing position after atropine. Combined blockade allowed for differentiation of the mechanical effects of respiration on arterial pressure from the indirect effect of respiration on arterial pressure through HR [via the respiratory sinus arrhythmia (RSA)].

Data analysis. The ECG, ILV, and arterial pressure signals were sampled and analyzed off-line on a computer (Masscomp MC-500). After antialias filtering at 180 Hz with eight-pole Butterworth filters, all the signals were sampled at 360 Hz. R waves were detected from the ECG, and a smoothed instantaneous HR time series was constructed at 3 Hz (10). The ILV and arterial pressure signals were digitally filtered and decimated to 3 Hz. This 3-Hz representation of the arterial blood pressure signal will be referred to as ABP. Systolic and diastolic pressures (SBP and DBP) were identified from each beat of the nondecimated arterial pressure signal, and the values were splined and sampled at 3 Hz so that values of all the constructed time series occurred simultaneously. A pulse pressure (PP) signal was formed by subtracting DBP from SBP. Two ~6 min (341 s = 1,024 points) segments of data were chosen for analysis from each 13-min record of random interval breathing. Power spectra of the HR, ILV, ABP signal, and derived blood pressure signals (SBP, DBP, and PP) for each 6-min segment were estimated using the Blackman-Tukey method. Representative time series and spectra of all the signals from one subject in the supine position before

autonomic blockade are shown in Fig. 1. The random interval nature of the respiratory signal is evident both in the ILV time series and its spectrum (Fig. 1A). Note how the frequency content of the HR and arterial pressure signals are subsequently broadened. ILV and HR time series and spectra from a subject breathing at a fixed frequency are included for comparison (Fig. 1, F and G). The cross-spectra between ILV and HR, between ILV and each arterial pressure signal, and between HR and each arterial pressure signal were also computed for each data segment. The complex transfer functions (or frequency response) for each relationship, $H(f)$, and their magnitudes and phases, $|H(f)|$ and $\theta(f)$ were then estimated using the cross-spectral method as previously described (11). The squared coherence function, $\gamma^2(f)$, which ranges between 0 and 1, was used to assess the statistical reliability of the transfer function estimates at each frequency (11). A value of unity indicates a perfectly linear relationship between the input and output at that frequency.

The transfer phase will yield a negative value of θ when changes in the input precede changes in the output (40). Thus we define a phase lag between the input and output as a value of θ below 0° and a phase lead as θ above 0°. We have defined zero phase as synchrony between inspiration and rising heart rate or increasing ABP. The mean and standard deviation of the HR, ABP, SBP, DBP and PP signals for each data segment were also calculated.

Statistical analysis. Group-average transfer function magnitude and phase estimates and their associated standard errors were computed using data from corresponding epochs across the fourteen subjects, using the method described in detail in APPENDIX B (see *Eqs. B5* and *B9*). Data from all 14 subjects were pooled to obtain group-average transfer function estimates for the supine control, standing control, supine double blockade, and standing double blockade states. Data from the seven subjects who received atropine first were used to compute the average transfer functions for the supine and standing vagal blockade states. Similarly, data from the seven subjects given propranolol first were pooled to obtain
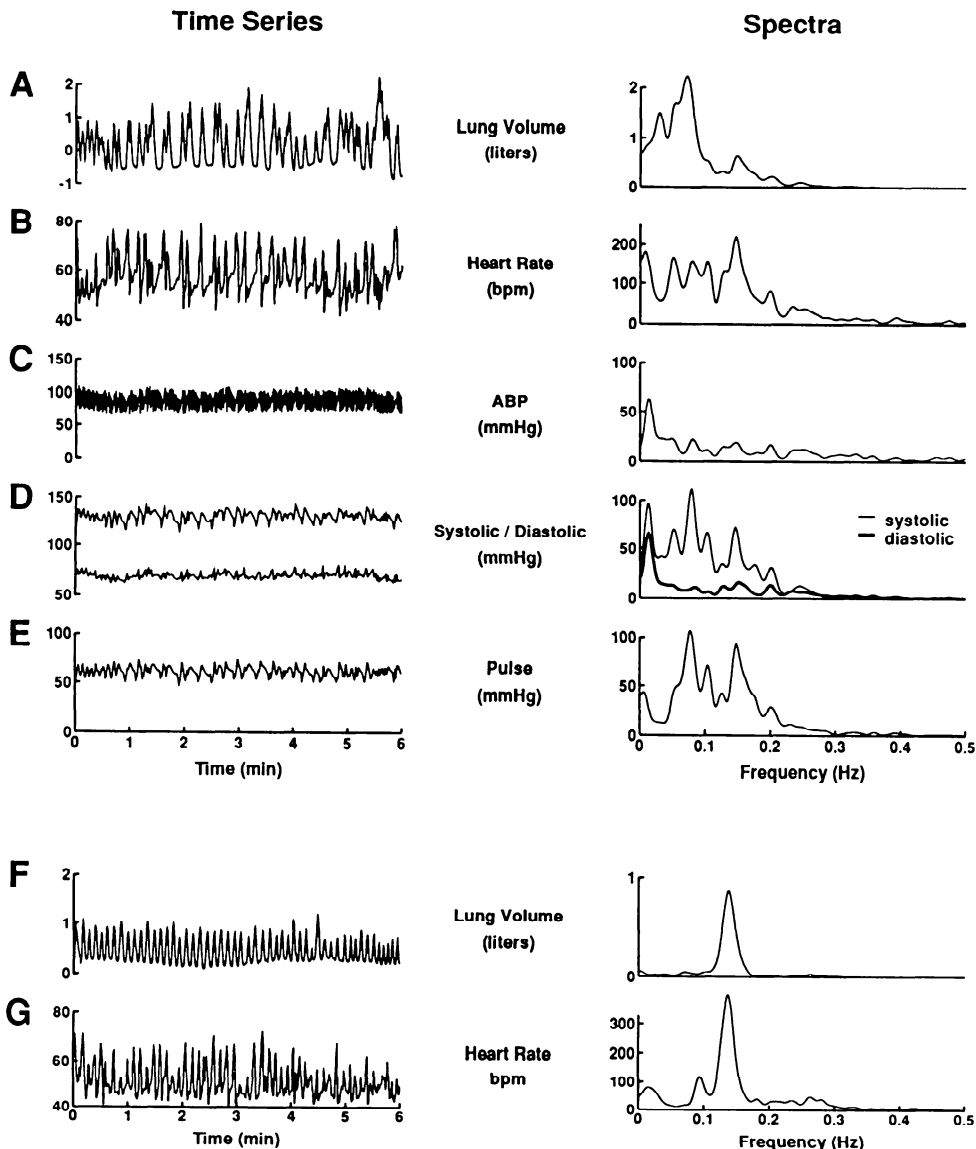
Time Series

Spectra

FIG. 1. Representative time series and spectra (*A–E*) of instantaneous lung volume, heart rate, a filtered 3-Hz representation of arterial blood pressure (ABP), and systolic, diastolic, and pulse pressures from 1 subject. Random interval breathing (*A*) broadened frequency content of all signals, producing spectra with significant magnitude at most frequencies between 0 and 0.5 Hz and few discrete peaks. Systolic pressure fluctuations were generally larger than diastolic pressure fluctuations, as both time series and spectra (*D*) show in this subject. Spontaneous breathing (*F*) in a different subject produced a large peak in HR power spectrum at primary respiratory frequency plus some smaller lower frequency peaks.

group-average estimates for the supine and standing sympathetic blockade states.

Standard errors and significance levels were computed for all group-average transfer function comparisons using Eqs. B6 and B10 in APPENDIX B, but error indicators are not presented in some figures with multiple plots to avoid confusion. The Student's unpaired t test was used to determine whether two group-average transfer function magnitudes or phases were significantly different at each frequency from 0 to 0.5 Hz. $P < 0.05$ was considered significant. The Student's paired t test was used to assess differences in the HR, ABP, SBP, DBP, and PP means and variances from different physiological states. Again, $P < 0.05$ was considered significant.

RESULTS

Autonomic mediation of RSA. Representative time series, power spectra, and transfer functions for the HR and ILV signals from *subject 1* during vagal conditions (supine + propranolol), and from *subject 2* during sympathetic conditions (standing + atropine) are displayed in Fig. 2. The ILV signals (Fig. 2, *A* and *G*) clearly demonstrate the random interval nature of the respiratory pattern. Although the absolute magnitude of the

power in the spectrum of the respiratory signal from *subject 1* (Fig. 2*C*) is much lower than that of *subject 2* (Fig. 2*I*) because of smaller individual breaths, the respiratory power spectra of both subjects demonstrate broadened frequency content compared with spontaneous breathing. In contrast, the corresponding HR spectra (heavy lines of Fig. 2, *C* and *I*) demonstrate relatively broad frequency content for the vagal case but virtually no power above 0.1 Hz for the sympathetic case. The magnitude and phase of the transfer functions between ILV and HR also display clear differences between the sympathetic and vagal responses. Vagal HR control is characterized by only a small decrement in magnitude with frequency and near zero phase at frequencies from 0 to 0.5 Hz (Fig. 2, *D* and *E*), whereas sympathetic HR control is characterized by markedly reduced gain above 0.1 Hz and phase that approaches 180° at DC, with a progressive phase delay from ILV to HR as frequency increases (Fig. 2*J* and *K*). The coherence spectra (Fig. 2, *F* and *L*) are near or above 0.5 throughout at most frequencies above 0.1 Hz, indicating that the magnitude and phase estimates are relatively reliable at those frequencies. It is important to note that despite the fact that *subject 2* has much more low frequency HR power than *subject 1*, the transfer function, which effectively
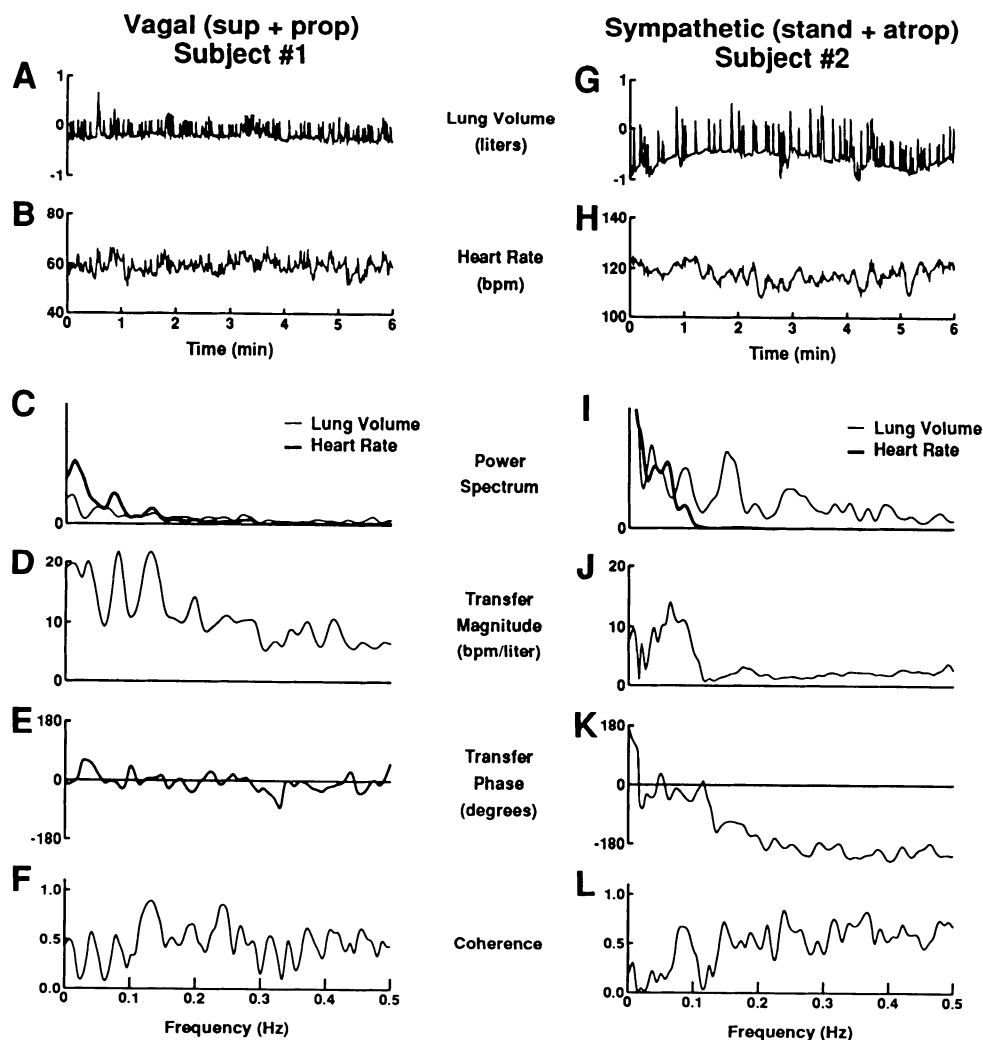

FIG. 2. Representative data for respiratory sinus arrhythmia from 1 subject in vagal state (*A-F*) and 1 in sympathetic (*G-L*) state. Shown are instantaneous lung volume (ILV) and heart rate time series (*A, B, G,* and *H*), respiratory and heart rate power spectra (*C* and *I*), transfer function magnitude (*D* and *J*) and phase (*E* and *K*) spectra, and coherence functions (*F* and *L*). Spikes in 6-min lung volume time series (*A* and *G*) are individual breaths. Intervals between them vary randomly, resulting in broadband power in lung volume spectra (narrow lines, *C* and *I*). Y-axis scale for the lung volume spectra is 0 to 0.2 l²/Hz. Y-axis scale for the heart rate spectra (thick lines, *C* and *I*) is 0 to 100 bpm²/ Hz. (bpm = beats/minute). Note that the ILV time series and corresponding power spectrum have a smaller amplitude for *subject 1* than for *subject 2*. Despite the difference in the ILV input, reliable transfer function estimates were obtained in both subjects.

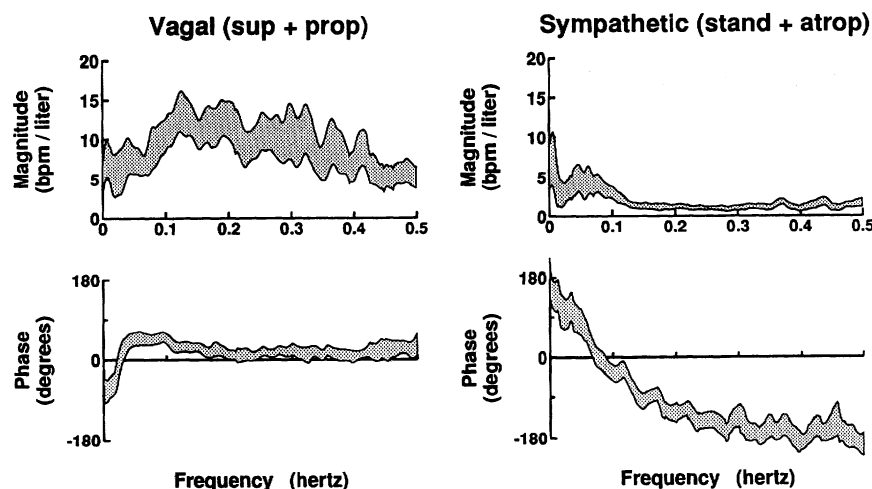## Vagal (sup + prop)

Sympathetic (stand + atrop)

FIG. 3. Instantaneous lung volume-heart rate relations (respiratory sinus arrhythmia, RSA). Group-average transfer function magnitude and phase spectra between lung volume and heart rate (RSA) for vagal (supine + propranolol) and sympathetic (upright + atropine). Gray area encloses means ± SE.

normalizes the HR output for a larger respiratory input, actually has a higher low frequency magnitude for *subject 1*.

Group-average transfer function magnitudes and phases (Fig. 3) showed similar results to those for the individuals in Fig. 2. The confidence zones, representing the standard error of the mean, indicate that the magnitude estimate for the group is significantly less ($P <$ 0.05) for sympathetic compared with vagal HR control at all frequencies above 0.07 Hz. The phase estimates are significantly different ($P <$ 0.01) at all frequencies between 0 and 0.5 Hz except where the two averages cross near 0.06 Hz. The shapes are also very different and are consistent with the individual data shown in Fig. 2. At most frequencies, the vagal HR response to respiration is characterized by near zero but slightly positive phase, indicating that the HR response actually leads the changes in ILV by a very small amount. The sympathetic HR response starts at 180°, indicating that at

very low frequencies HR decreases with increases in ILV (inspiration) and then falls with frequency, indicating an increase in the phase lag between changes in the ILV signal and changes in HR as frequency increases. It should be noted, like the ILV-HR transfer function for *subject 1* in Fig. 2, the magnitude of the group-average vagal transfer function actually has a maximum near 0.15 Hz and then falls with frequency above 0.15 Hz.

Figure 4 compares the pure vagal and pure sympathetic ILV-HR average transfer functions without error bars with the ILV-HR transfer functions in the mixed autonomic states of supine and standing control (without autonomic blockade). Qualitatively, certain aspects of both the vagal and sympathetic relations can be seen in the supine and standing relations. The precise mix of the two autonomic components is addressed quantitatively through the results of the model presented in the APPENDIX A.

Respiratory influences on arterial pressure. With sub-
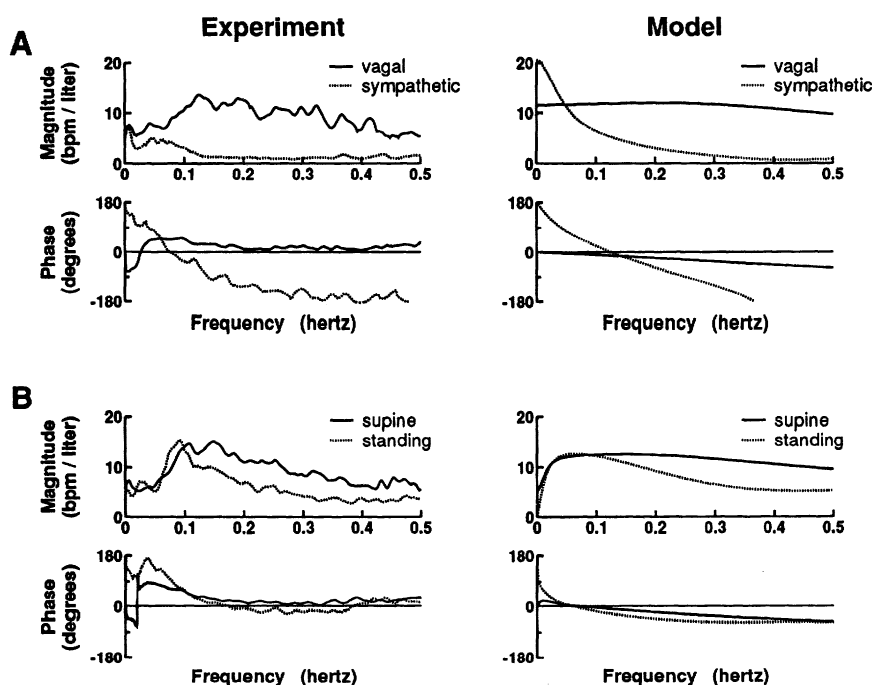
Experiment

Model

FIG. 4. Instantaneous lung volume-heart rate (HR) relations (RSA). Experimental (group average) and analytic (model of Fig. 9, see APPENDIX A) transfer relations between respiration and HR (H_{rh}) for vagal and sympathetic states (A) and supine and upright states (B). For simplicity SE indicators as in Fig. 3 are omitted. See text for discussion of significance.
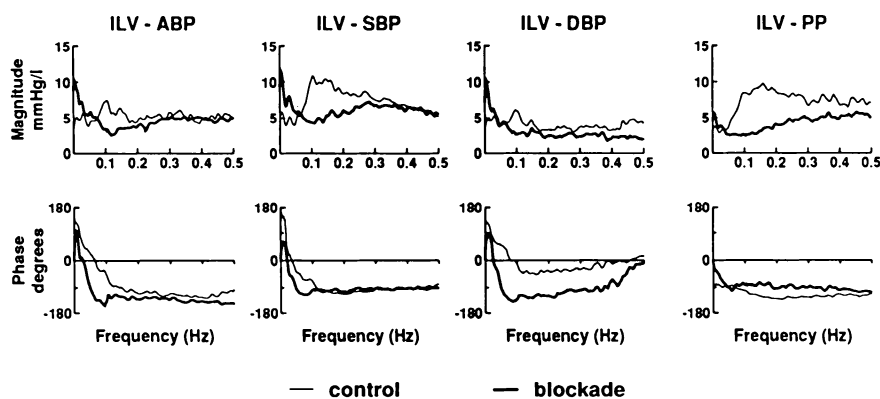
FIG. 5. Instantaneous lung volume (ILV)-ABP relations for control vs. blockade. Group average magnitudes and phases for transfer functions between ILV and ABP, systolic (SBP), and diastolic (DBP) blood pressures, and pulse pressure (PP) for all 14 subjects in supine position. Heavy lines represent data after combined vagal and β-adrenergic blockade. For simplicity SE indicators are omitted. See text for discussion of significance.

jects in the supine position, before autonomic blockade when neural HR control was intact (HR variance = 38.8 ± 23.7 beats/min^2) and after combined autonomic blockade when HR fluctuations were virtually eliminated (HR variance = 1.2 ± 0.5 beats/min^2), the magnitude of the group-average transfer function from ILV to SBP was significantly greater than that to DBP at frequencies above 0.07 Hz (Fig. 5). Combined autonomic blockade significantly decreased the transfer function magnitude between ILV and both SBP and PP at frequencies between 0.05 and 0.25 Hz but did not significantly affect the transfer magnitude between ILV and DBP or ILV and ABP. Above 0.25 Hz, neither the transfer magnitude nor phase was significantly changed by combined autonomic blockade.

We noted that after blockade at frequencies above 0.1 Hz, the transfer magnitude from ILV to PP increased nearly linearly with frequency and the phase remained very close to −90° so that the magnitude and phase were similar to those of a differentiator in series with an inverter (Fig. 5). We speculate that the negative differentiator nature of the ILV-PP transfer relation was present because ILV-PP most faithfully reflected the mechanical coupling between ILV and arterial pressure
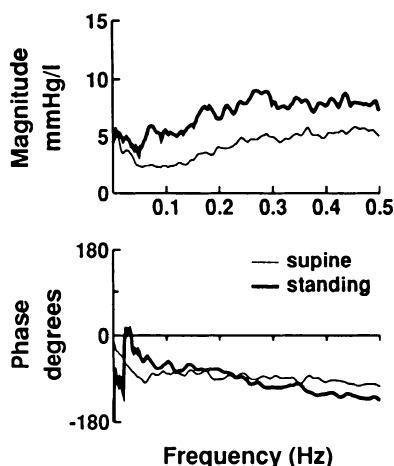

FIG. 6. ILV-PP relations (blockade) for supine vs. upright. Group-average transfer magnitudes and phases for mechanical coupling between ILV and PP for all 14 subjects after combined blockade in supine and upright posture. Heavy lines represent data in subjects in upright posture. For simplicity SE indicators are omitted. See text for discussion of significance.

(see DISCUSSION). Therefore, to further analyze the influence of posture on the mechanical effects of ILV on arterial pressure, the ILV-PP transfer function for the supine combined blockade state shown in Fig. 5 is replotted in Fig. 6 with the corresponding transfer relation for the standing combined blockade state. With subjects in the upright posture, the transfer magnitude between ILV and PP was significantly higher than in the supine posture, indicating that the mechanical coupling between respiratory activity and the vasculature within the thorax is stronger in the standing than the supine position. However, with subjects in the upright posture, the ILV-PP transfer magnitude rises less linearly with frequency than in the supine case, possibly reflecting the presence of additional nonderivative mechanisms which contribute to the mechanical coupling between ILV and arterial pressure.

All of the changes noted above that occurred with combined blockade were nearly identical to those that occurred after vagal blockade with atropine alone. In addition, selective sympathetic blockade with propranolol did not significantly change any of the transfer relations between ILV and the various arterial pressure signals (not shown). Thus the sympathetic nervous system did not contribute significantly to the influence of respiration on arterial pressure.

Respiratory influences on HR-combined blockade. When autonomically mediated HR fluctuations should have been eliminated after combined blockade with both propranolol and atropine, the transfer relation between ILV and HR still had a very small but identifiable magnitude that increased linearly with frequency at frequencies above 0.15 Hz. The phase was very close to 90° at the same frequencies (Fig. 7). Importantly, despite the relatively small magnitude, the standard error bars for both the magnitude and phase indicate that the response was very consistent among the subjects and suggests a common mechanism. As with the transfer relation between ILV and PP, these characteristics are very similar to those of a derivative function, suggesting that there is a nonautonomic HR control mechanism which is closely related to the rate of change of lung volume or respiratory airflow.

ABP-HR transfer relations. When the arterial baroreceptor-HR reflex is intact, the relationship between ABP and HR is closed loop; i.e., HR affects ABP through the
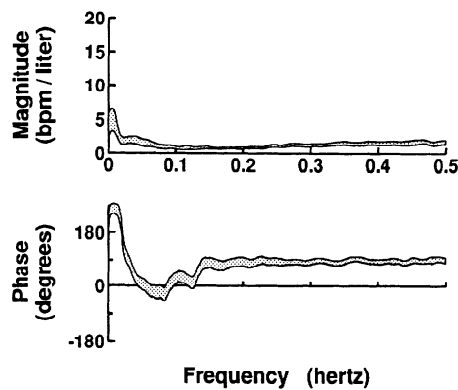
FIG. 7. ILV-HR relations (blockade). Group average transfer function magnitude and phase between ILV and HR (RSA nonautonomic) after combined autonomic blockade in supine position. At frequencies above 0.15 Hz magnitude is small but increases linearly with frequency while phase is very close to 90°. Together these findings are consistent with nonautonomic changes in HR, which are proportional to derivative of instantaneous lung volume (respiratory flow). Gray area includes means ± SE.

mechanical coupling between the left ventricle and the vasculature, and ABP affects HR through the baroreflex. Transfer functions such as we have calculated do not build in causality and simply represent the magnitude and phase relationship between the two signals. Thus the transfer function between ABP and HR cannot be interpreted as characterizing either the mechanical feedforward from HR to ABP or the baroreflex feedback from ABP to HR. Figure 8 presents the results for control conditions in the supine and standing positions and for the pure vagal and pure sympathetic states. The magnitude of the transfer relation between the ABP signal and HR was significantly lower in the standing than the supine position at frequencies above 0.1 Hz (Fig. 8B). The phase relations were similar in both positions, except at frequencies below 0.1 Hz.

Of note, in the mixed autonomic states of supine and standing control the phase at most frequencies is neither near 0° as one might expect for the feedforward from HR to ABP nor near 180° as one might expect for the feedback from ABP to HR. This fact demonstrates that the ABP-HR relationship is influenced by the interactions between both the feedforward and feedback pathways and does not characterize either pathway alone.

Responses of mean and variance: HR and ABP. Table 1 gives the mean of the HR, ABP, SBP, DBP, and PP signals and the variance of all except the ABP signal for each autonomic condition. For digital signal processing purposes, one must choose a frequency to represent the true arterial blood pressure signal. We chose 3 Hz, a choice that requires restriction of the frequency content of the ABP signal to the Nyquist frequency, 1.5 Hz. When the mean HR is near or above 1.5 Hz (90 beats/min), the pulsatile nature of the arterial pressure signal, which is responsible for much of the variance in the signal, will no longer be represented in our ABP signal. Thus the variance of the ABP signal is highly dependent on the mean HR, provides no useful physiological information, and is not presented.

Mean HR significantly increased with a change in position from supine to standing during control conditions (+11.6 beats/min, $P < 0.0005$) and after either sympathetic (+7.8 beats/min, $P < 0.005$) or vagal (+11.1 beats/min, $P < 0.05$) blockade but actually decreased slightly (NS) with the change to standing position after combined blockade (−1.7 beats/min). Propranolol alone significantly decreased supine HR by 9.3 beats/min ($P < 0.002$) and standing HR by 11.6 beats/min ($P < 0.0005$), whereas atropine alone increased supine HR by 36.8 beats/min ($P < 0.0005$) and standing HR 32.9 beats/min ($P < 0.05$) (compared with control conditions for the 2 sets of 7 subjects). The supine intrinsic HR (after combined blockade) for all 14 subjects was 94.6 beats/
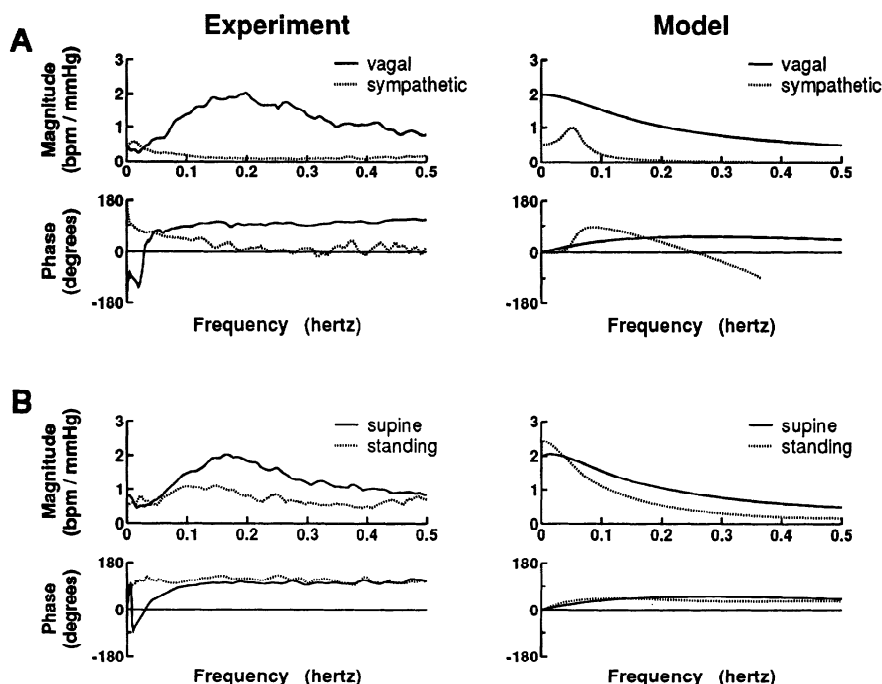

FIG. 8. ABP-HR relations. Experimental (group average) and analytic (model of Fig. 9, see APPENDIX A) transfer relations between ABP and HR (H_{bh}) for vagal and sympathetic states (*A*) and supine and upright states (*B*). For simplicity SE indications are omitted. See text for discussion of significance.

TABLE 1. *Means and variances*

	Control (n = 14)		Atropine (n = 7)		Propranolol (n = 7)		Combined (n = 14)	
	Supine	Standing	Supine	Standing	Supine	Standing	Supine	Standing
Means								
HR, beats/min	69±9	82±9*	109±16†‡	120±15*†‡	58±6†‡	66±6*†‡	95±11†	93±7†
ABP, mmHg	89±8	87±13	98±13§	93±12	90±10‡	87±20	103±12	90±14*†
SBP, mmHg	133±13	124±15*	139±17	126±18*	129±17‡	119±22	143±18	120±17*
DBP, mmHg	70±7	72±12	83±10†	79±10	72±8‡	72±18‡	84±11§	77±14†
PP, mmHg	63±13	52±8*	56±8	47±12*	56±12	48±10*	59±11	43±8*†
Variances								
HR, (beats/min)^2	39±25	50±23	5±8†	9±3†	31±30‡	25±29†‡	3±3‡	5±3†
SBP, mmHg^2	28±15	71±28*	34±30	79±23*‡	22±4	35±16*†	21±5	44±17*†
DBP, mmHg^2	12±3	24±8*	15±9	40±12*†	13±8	14±3†‡	13±12	29±13*†
PP, mmHg^2	16±11	37±19*	15±16	25±8*‡	12±7	17±11†	7±7†	16±9*†

Values are means ± SD. HR, heart rate; ABP, SBP, DBP, arterial, systolic, and diastolic blood pressures; PP, pulse pressure. * Vs. supine, $P < 0.05$. † Vs. control, $P < 0.05$. ‡ Vs. double, $P < 0.05$.

min.

The HR variance did not change significantly when subjects were moving from supine to standing under any conditions. Vagal blockade with atropine significantly decreased the HR variance compared with either control conditions or existing sympathetic blockade in both postures. In contrast, sympathetic blockade alone significantly decreased the HR variance only in the standing position and caused no change in the supine position.

Mean arterial pressure, represented by the mean value of ABP, did not significantly change with a shift in posture from supine to standing during control conditions or after either sympathetic or vagal blockade but did increase ($P < 0.008$) with the change to the standing position after combined blockade. SBP decreased after a shift from supine to standing under all conditions, but DBP did not significantly change during any condition. Thus PP decreased after a shift from supine to standing under all conditions. Propranolol alone or after vagal blockade with atropine caused no significant change in the average value of any arterial pressure variable during any condition in either posture. In subjects in the supine position, atropine alone or after sympathetic blockade with propranolol generally caused an increase in all the arterial pressure signals except PP, which decreased. However, in standing subjects, atropine did not significantly change any pressure variable during its addition to existing sympathetic blockade. Like atropine, double blockade generally led to an increase in ABP, SBP, and DBP and a decrease in PP, but unlike the response to atropine, the findings were consistent in both postures.

The variance of the SBP, DBP, and PP signals increased after a shift from supine to standing during all conditions except sympathetic blockade, when DBP did not change. With subjects in the supine position, there were no significant changes in the variance of SBP or DBP with any intervention; however, with subjects in the standing position the variance of SBP and PP decreased with propranolol alone or with the addition of propranolol to vagal blockade. Changes in the variance of other pressure variables while standing were small and inconsistent.

DISCUSSION

Autonomic mediation of RSA. In a previous study (40), we demonstrated in humans that the magnitude and phase characteristics of the system which generates the RSA can be efficiently determined over a range of physiologically important frequencies through the use of a broad-band respiratory input. We also speculated on the autonomic mechanisms involved in the mediation of the RSA based on 1) the changes we observed in the transfer function between ILV and HR with a change in position from supine to standing and 2) the results of a computer model that included data from animal experiments describing the transfer characteristics of the sinoatrial (SA) node in response to modulation of cardiac vagal and sympathetic activity (11). The results of the present study confirm that both cardiac parasympathetic and sympathetic activity are important in modulating HR in response to respiratory activity (RSA) and that the phase and magnitude characteristics of the ILV to HR transfer function can be used to identify the role of each branch of the autonomic nervous system in mediating the response. Specifically, between 0 and 0.5 Hz, vagal HR control is characterized by a maximum gain near 0.15 Hz, a small decrease in gain with frequency above 0.15 Hz, and no significant phase delay between ILV and HR.

In contrast, sympathetic HR control is characterized by lower gain than that for vagal control at frequencies below 0.1 Hz, markedly reduced gain at frequencies above 0.1 Hz, and phase that approaches 180° at DC with a progressive phase delay from ILV to HR as frequency increases (Fig. 3). These characteristics for vagal and sympathetic HR control are nearly identical to those we obtained with direct modulation of cardiac vagal and sympathetic nerve activity in dogs (11), with the exception of a 180° phase shift or an inversion. Thus our findings indicate that RSA is due to respiratory modulation of both cardiac sympathetic and vagal efferent nerve activity, but with an inversion due to suppression of both vagal and sympathetic outflow with inspiration. The HR response is then determined almost entirely by

the response characteristic of the SA node.

Although no previous investigator has examined autonomic mediation of RSA in a similar way, many investigators have attempted to either describe the phenomenological characteristics of the RSA or understand the relationship of cardiac vagal efferent activity to the RSA (3, 7, 16, 17, 19, 22, 24, 29, 30, 33). Those who have examined the dependence of the magnitude of the RSA on the respiratory frequency have found that the change in HR per unit change in lung volume decreases as the respiratory frequency increases above 0.1 Hz (3, 17, 24). Such a finding is in complete agreement with the ILV to HR transfer functions that we computed under both control conditions and sympathetic blockade (vagal conditions). In fact, Hirsch and Bishop (24) found that the corner frequency for the roll-off in gain was ~0.1 Hz and found a maximum magnitude of 15 beats·min^{-1}·l^{-1}. Angelone and Coulter (3) found similar characteristics for their ILV-HR transfer function and, in complete agreement with our data, found a dip in magnitude at very low frequencies around 0.05 Hz and a change in phase with frequency. Eckberg (19), who also examined the phase relation between respiration and HR, found that HR increases during the inspiratory phase of respiration (i.e., a 0° phase lag) at typical respiratory frequencies of ~0.2 Hz (12 breaths/min) but that the same relationship was not necessarily true at lower and higher respiratory frequencies. Such findings are entirely consistent with our previous data in supine and standing humans without autonomic blockade; however, our current data strongly support a new explanation for these findings.

Eckberg (19) attributed this phase relation to a frequency-dependent change in the relation between respiratory activity and vagal efferent activity. However, the transfer functions that we obtained clearly demonstrate that, under pure vagal conditions (Fig. 3), the phase lag from ILV to HR is near 0° at all frequencies, indicating that HR always increases during inspiration and decreases during expiration. Alternatively, under pure sympathetic conditions the phase relation (Fig. 3) indicates that HR tends to decrease with inspiration, but with a delay of between 3 and 5 s, so that the phase relationship starts out at −180° at 0 Hz and crosses 0° at ~0.1 Hz. These results provide a basis for understanding the phase and magnitude characteristics of the RSA that we and others have observed when HR is under both vagal and sympathetic control. During the mixed autonomic states of supine and standing control conditions in this study, the transfer phase and magnitude relations between ILV and HR have features which resemble both the vagal and sympathetic states (Fig. 4). At frequencies above 0.15 Hz, the transfer magnitude is lower in subjects in the standing than the supine position and the phase is near 0° in both positions. These findings indicate that, in both postures, RSA at frequencies above 0.15 Hz is predominantly mediated through modulation of vagal activity but to a lesser degree in the standing position. At frequencies below 0.15 Hz, the transfer magnitude is nearly identical in the two positions, but in subjects in the standing position the phase approaches 180°. These findings suggest that in subjects in the standing position, the

reduction in vagal modulation of HR, which should decrease the transfer function magnitude at all frequencies, is balanced by an increase in sympathetic modulation of HR, which selectively augments the transfer magnitude at low frequencies. To further demonstrate how both vagal and sympathetic activity modulate HR, we designed a model that uses a weighted linear combination of the open-loop vagal and sympathetic transfer functions of the SA node to predict the magnitude and phase of the RSA (see APPENDIX A). The model mimics the experimental results in both pure and mixed autonomic states further supporting the above hypotheses and also supporting the notion that the frequency dependence of the RSA is a result of the transmission characteristics of the SA node in response to inverted modulation of vagal and sympathetic activity by respiration.

Respiratory influences on arterial pressure. Our findings indicate that in humans fluctuations of arterial pressure which occur with respiration are due to both the mechanical thoracic coupling between respiration and the vasculature and the effects of respiratory induced fluctuations of HR (RSA). At frequencies between 0.05 and 0.25 Hz, the transfer magnitude from ILV to SBP and PP decreased but remained greater than zero, with the elimination of most HR variability by complete autonomic blockade (Fig. 5). This finding indicates that some, but not all, of the respiratory variance in arterial pressure is due to HR variability. Above 0.25 Hz, neither the magnitude nor phase between ILV and SBP or PP was significantly affected by autonomic blockade, strongly suggesting that at higher frequencies RSA plays little role in mediating arterial pressure fluctuations. Previous studies examining these issues have been controversial. Akselrod et al. (1) concluded that, in resting conscious dogs, respiratory induced fluctuations of arterial pressure are due almost entirely to HR fluctuations at the respiratory frequency. DeBoer et al. (18) concluded that the opposite was true in a sitting human breathing at ~0.25 Hz; i.e., respiration mechanically influences cardiac output which changes arterial pressure and finally influences HR through the effects of the baroreflex on vagal activity. Although the closed-loop nature of the interaction between HR and arterial pressure makes quantitative conclusions on the relative weight of the mechanical vs. the autonomic effects (RSA) of respiration on pressure difficult to draw, our data clearly indicate that in supine humans both effects are significant at frequencies below 0.25 Hz. Alternatively, above 0.25 Hz, our data suggest that the mechanical influence of respiration on arterial pressure dominates the influence of RSA. Thus our findings are entirely consistent with DeBoer et al.'s conclusion, formed from data in sitting humans breathing at a single high respiratory frequency; i.e., at higher frequencies respiration primarily affects arterial pressure, which then elicits buffering of this effect through the HR baroreflex. Furthermore, we found that during combined blockade the pure mechanical influences of respiration on arterial pressure, as illustrated by the effect on PP, were larger in the standing than the supine position and that the magnitude of the mechanical effects increased with increasing frequency (Figs. 5 and 6). It

thus appears that the physiological link between respiration and arterial pressure is dependent on multiple factors, which include species, posture, or hemodynamic stress and the respiratory frequency.

These conclusions can account for the findings of DeBoer et al. (18) and Akselrod et al. (1) and offer considerable insight into short-term arterial pressure control. When HR fluctuations arise from direct central nervous modulation of autonomic activity and are large, such as occurs in the normal resting dog (HR may vary as much as 50 beats/min with each breath), the feedforward from HR to arterial pressure is most important in determining short-term arterial pressure variability. Alternatively, when HR fluctuations are smaller, such as is the case with RSA in humans (particularly while standing) and when mechanical influences are larger, such as occurs in either the standing position or at a higher respiratory rate, the mechanical influences of respiration on arterial pressure may dominate and secondarily influence HR through the arterial baroreflex. In addition, our finding that sympathetic blockade did not significantly change the respiratory-arterial pressure transfer relations, either before or after parasympathetic blockade, suggests that in both supine or standing humans sympathetic modulation of HR by respiration is not large enough to significantly influence arterial pressure.

The pure mechanical effect of ILV on the arterial pressure signals (combined blockade) was smaller for DBP than SBP and, except at very low frequencies below 0.05 Hz, behaved very much like a negative differentiator for PP. This differentiator effect indicates that changes in PP were more closely related to the negative rate of change of ILV, i.e., respiratory flow, than to the ILV itself. We speculate that the pure mechanical effects of ILV on arterial pressure were best represented by ILV-PP because both SBP and DBP were similarly "contaminated" by other arterial pressure control mechanisms such as peripheral vascular resistance. Subtracting DBP from SBP to obtain PP effectively eliminates these other influences.

Jurgen et al. (26–28) have examined extensively the normal fall in both arterial pressure and left ventricular stroke volume that occurs with an inspiratory decrease in intrathoracic pressure and have concluded that the phenomenon is due to independent effects of negative intrathoracic pressure on both left ventricular preload and afterload. They suggested that decreased preload results from increased right ventricular filling, which leads to a pericardial constraint and a decrease in diastolic left ventricular compliance and filling or "ventricular interdependence" (26), whereas increased afterload results from an increase in transmural left ventricular pressure. They also found that the application of negative intrathoracic pressure led to an increase in aortic cross-sectional area, a reduction in thoracic aortic pressure, and a reduction in antegrade flow, or even retrograde flow, in the descending aorta (27, 28). This last finding supported a mechanism for inspiratory reductions in ABP which Olsen et al. (36) referred to as a "reverse thoracic pump." Our findings do not differentiate the relative effects of changes in preload or afterload with respiration but add clarity to the nature of the physical link between respiratory activity and the thoracic vasculature.

Whether the changes in PP are due to changes in ventricular filling or ejection, we found that the effect is strongest during maximal respiratory flow when intrathoracic pressure is changing fastest (43), not at peak inspiration. Once inspiratory effort ceases, intrathoracic pressure reaches a new steady state, determined by the elastic recoil properties of the lung. Because PP changes seem to be related to the rate of change of intrathoracic pressure, we hypothesize a type of capacitive coupling between the intrathoracic space and the arterial and venous thoracic vasculature. The mechanism for the changes in vascular pressure with inspiration is charging of the thoracic arterial and venous capacitors with blood from the extrathoracic arterial and venous capacitors, as documented by Jurgen et al. in the aorta (27, 28). Although not noted by Jurgen et al. (27), their Fig. 3 clearly demonstrates that retrograde descending aortic flow during diastolic phrenic nerve stimulation is related to the rate of change rather than the actual value of esophageal pressure, which was used as a reflection of intrathoracic pressure. Such a capacitive coupling can account for the derivative effect of respiration on PP and helps explain the larger effect of respiration on SBP than DBP.

During systole when the aortic valve is open, intrathoracic pressure mediates its direct effect on ABP through the combined capacitance of both the thoracic arterial vasculature ($C_{A,thor} \sim 1$ ml/mmHg) and the ventricle (mean $C_{vent,sys} \sim 0.75$ ml/mmHg), whereas during diastole only $C_{A,thor}$ is involved. Thus, from this mechanism, the effect on SBP is expected to be approximately twice that on DBP, and the effect should increase in magnitude with increasing frequency. Clearly, changes in ventricular filling and stroke volume with respiration play a role in modulating arterial pressure that is not accounted for in this explanation. In fact, during inspiration an increase in right ventricular filling, which leads to a decrease in left ventricular filling through ventricular interdependence, may also affect SBP more than DBP.

Thus our findings are most consistent with a model in which the respiratory changes in arterial pressure are due at least partially to the capacitive coupling between intrathoracic pressure variations and the left ventricle and thoracic arterial vasculature. Our model may have implications for the management of conditions that accentuate the normal inspiratory fall in arterial pressure, such as asthma, pulmonary edema, or cardiac tamponade. Because the arterial pressure changes are most closely related to the rate of change of lung volume, slower deeper breaths are most likely to minimize the hemodynamic effects of respiration even if the minimum and maximum values of intrathoracic pressure are unchanged.

ABP-HR relations. As previously noted, our transfer functions between ABP and HR represent the combined effects of the HR baroreflex and the mechanical feedforward from HR to ABP and do not necessarily reflect the

open-loop characteristics of the HR baroreflex. In fact, the transfer functions differed substantially from the known open-loop behavior of the HR baroreflex. When operating in their steady-state linear regimes, the open-loop carotid and aortic arch baroreflexes produce a step change in HR in the opposite direction of a preceding step change in ABP (2, 41). Such a relationship corresponds to a 180° phase shift between ABP and HR (i.e., out of phase) as the frequency of the changes in ABP approaches 0 Hz, (i.e., when the fluctuations of ABP occur sufficiently slowly that any delays in the HR response are small compared to the cycle length of the ABP fluctuation). In this study during closed-loop operation, the phase approached 180° at 0 Hz only in the sympathetic control state (Fig. 8A). During the other three sets of conditions, all of which were characterized by a higher transfer magnitude than the sympathetic state, the phase was inconsistent at low frequencies. At frequencies >0.1 Hz, the phase hovered between 0 and 180°. Although difficult to account for precisely, these findings can be understood by realizing that during closed-loop operation, the relationship between ABP and HR reflects both the feedback from ABP to HR through the baroreflex, and the moderating influence that HR has on this response by changing ABP through changes in cardiac output. Unless the analysis scheme chosen can separately identify the feedforward and the feedback mechanisms between ABP and HR (5, 8), one must be very careful interpreting the transfer relations between ABP and HR. The observed phase relation we found between ABP and HR is simply the phase that results from the closed-loop operation of the system and is not typically equivalent to the open-loop phase of either the feedforward or feedback path.

Although our results attest to the complexities of identifying open-loop system responses during closed-loop operation, they can be compared with the results of other investigators using different methods to identify the closed-loop gain of the arterial HR baroreflex. Most investigations in humans have examined only the magnitude of the HR baroreflex, assuming a 180° phase. These studies have generally produced average magnitude (gain) values between 5 and 20 ms/mmHg (using the change in R-R interval rather than HR) (37, 42). Our average values for the magnitude in the supine control condition are between 1 and 2 beats·min^{-1}·mmHg^{-1} depending on the frequency, with a peak magnitude at ~0.2 Hz (period ~5 s). Because the average HR was ~70 beats/min, our results are equivalent to an R-R interval response of between 8 and 16 ms/mmHg, clearly comparable to the findings of other studies.

Nonautonomic control of HR. The transfer relation between respiration and HR after complete autonomic blockade was clearly nonzero and had features that were qualitatively similar to those of a positive differentiator, i.e., increasing gain with frequency and phase near 90° (Fig. 7). As noted above, in a discussion of the mechanical effects of respiration on ABP, such features are consistent with an effect due to the capacitive coupling between intrathoracic pressure and vascular structures within the heart. In this case, the mechanically induced increase in

HR is associated with inspiration. We hypothesize that, in the absence of autonomic heart rate control, the relatively small effect of sinus node stretch on the SA nodal firing becomes evident. Identification of this mechanism has been documented experimentally in the isolated-perfused heart of animals (14), where it has been found that an increase in atrial stretch increases HR; however, Raeder et al. (39) found that only 0.03% of the HR variability above 0.1 Hz remained after bilateral vagotomy in anesthetized dogs undergoing positive-pressure ventilation. Although it is possible that our findings are due to incomplete autonomic blockade, we used doses of atropine and propranolol, which have been documented previously to eliminate virtually all HR changes in humans (25). Furthermore, the phase of the ILV-HR relation during combined blockade was unlike the phase during any of the other pure or mixed autonomic states.

Evidence for a nonautonomic RSA mechanism in humans has been found in patients after cardiac transplant, where an RSA magnitude of ~2 beats·min^{-1}·l^{-1} was observed at respiratory frequencies between 0.08 and 0.33 Hz (13). These authors hypothesized an atrial stretch mechanism to explain their data and also found that the magnitude of the HR change was increased with increasing frequency. Our data further support the existence of a nonautonomic mechanism in humans, and provide additional evidence for an atrial stretch mechanism through the differentiator properties we observed.

Conclusion. Using transfer function analysis in combination with random interval breathing to broaden the frequency content of respiration, we have been able to precisely and efficiently characterize the vagal, sympathetic, and mechanical influences of respiratory activity on HR and arterial pressure. Our findings indicate that *1*) respiratory modulation of HR (RSA) is mediated primarily by suppression of both cardiac vagal and sympathetic efferent activity with inspiration and *2*) respiratory modulation of arterial pressure is mediated by a combination of the effect of the RSA and the mechanical coupling between respiratory activity and the thoracic vasculature. We also found a small nonautonomic, presumably mechanical, effect of respiration on HR, which had not previously been well characterized in humans. These findings are supported by a simple closed-loop model of HR and arterial pressure control (APPENDIX A) and form the basis for quantitatively identifying the gain of the response of HR to modulation of sympathetic and vagal activity in individual patients.

We also examined the HR baroreflex by determining the closed-loop transfer relation between ABP and HR. The phases and magnitudes of the transfer functions that we found were both consistent with the findings of other investigators and in partial agreement with our simple closed-loop model based on experimentally derived open-loop transfer functions for the SA node, the mechanical influences of HR on ABP, and the arterial baroreceptors; however, as expected our nonparametric methods did not take into account causality in this closed-loop model and, consequently, could not identify the open-loop transfer characteristics of the feedback and feedforward paths between ABP and HR. A para-

metric model and system identification scheme might be better suited to identify the characteristics of the model blocks in closed-loop operation.

APPENDIX A

Model of Circulatory Control

To help clarify and test various hypotheses concerning the complex links between respiration, HR, and ABP during closed-loop cardiovascular regulation, we expanded a simple model of the RSA proposed in a previous paper (40) by including the HR baroreflex and the mechanical effects of respiration on ABP (Fig. 9). The heavy black box in Fig. 9 outlines the previous model. The changes effectively close the feedback loop between HR and ABP; however, the model remains relatively simple and continues to ignore significant aspects of hemodynamic regulation, such as the effect of modulation of peripheral vascular resistance via the baroreflex and the influence of cardiopulmonary receptors. The model is specifically designed to predict the magnitude and phase of the transfer relations between respiration and HR (H_{rh}), respiration and ABP (H_{rb}), and HR and ABP (H_{hb}) as a function of frequency given the transfer relations, time delays, and inversions of the various blocks in the model. The blocks in the model defined below have been determined from the results of previous experimental studies.

Central effect of respiration on vagal and sympathetic efferent activity. Direct neural recordings in animals and humans have shown that vagal and sympathetic efferent activity decrease ~0.5 s before the onset of inspiration (21, 30). For simplicity we chose to ignore the 0.5-s pure time lead included in the previous model (11) but included the more important inverter.

Mechanical effect of respiration on ABP. Based on the combined blockade data from this study, which are presented in the results, the coupling between ILV and ABP is modeled as a negative derivative so that changes in ABP are more closely related to respiratory flow rather than lung volume.

Feedforward from HR to ABP. Previous work from our laboratory has shown that the transfer function between ventricular rate and ABP over the frequency range of interest (0–1.0 Hz) has a constant magnitude and a fixed time lag of 0.42 s (9). Thus we modeled this block as a constant K_v in series

with a fixed delay T_v of 0.42 s. K_v, which includes the properties of the arterial vasculature, was allowed to change with posture. The delay element is implemented in the frequency domain as

$$H_{\text{delay}}(f) = e^{-j2\pi f \tau} \qquad (A1)$$

where $\tau = T_v = 0.42$ s.

Feedback from ABP to vagal and sympathetic efferent activity. Based on the data of Scher and Young (41), the baroreceptors and their link to vagal and sympathetic outflow in the brain stem were modeled with a constant magnitude K_b. Borst and Karemaker (15) have estimated the time for afferent neural transmission of baroreceptor activity and central processing in the brain stem in humans to be ~0.3 s. Thus a fixed delay T_b was also included in the baroreceptor block using Eq. A1. The baroreceptors are linked to sympathetic efferent activity with an inverter because an increase in ABP leads to sympathetic withdrawal and a decrease in HR. Few direct data exist describing this relationship as a function of frequency, but Scher and Young (41) examined the response of HR to changes in ABP using sinusoidal variations of ABP. They found that under baseline conditions the magnitude of the response was constant and the phase close to 0° for frequencies from 0.06 to 0.3 Hz. Their data suggested that any frequency dependence in the baroreflex at these low frequencies was due to the response characteristics of HR to the autonomic efferents rather than the link between the baroreceptors and the autonomic efferents.

Central nervous interactions. Because the model is completely linear, the interaction of the baroreceptors and respiration in the brain stem was modeled as a simple summation. Relative weight factors, A_p and A_s, represent the transfer relations between respiratory or baroreceptor drive and the modulation depth of vagal and sympathetic efferent activity. These factors were allowed to change with the given state of autonomic balance.

SA node. The SA node response characteristics were taken directly from previous work in our laboratory (11, 40). The transfer function between instantaneous vagal firing rate and the HR was modeled as a single-pole low-pass filter H_p in series with an inverter (since vagal parasympathetic stimuli decrease heart rate). The transfer relation between sympathetic activity and HR was modeled as a single-pole low-pass filter H_s in series with a pure delay T_s of 1.7 s.
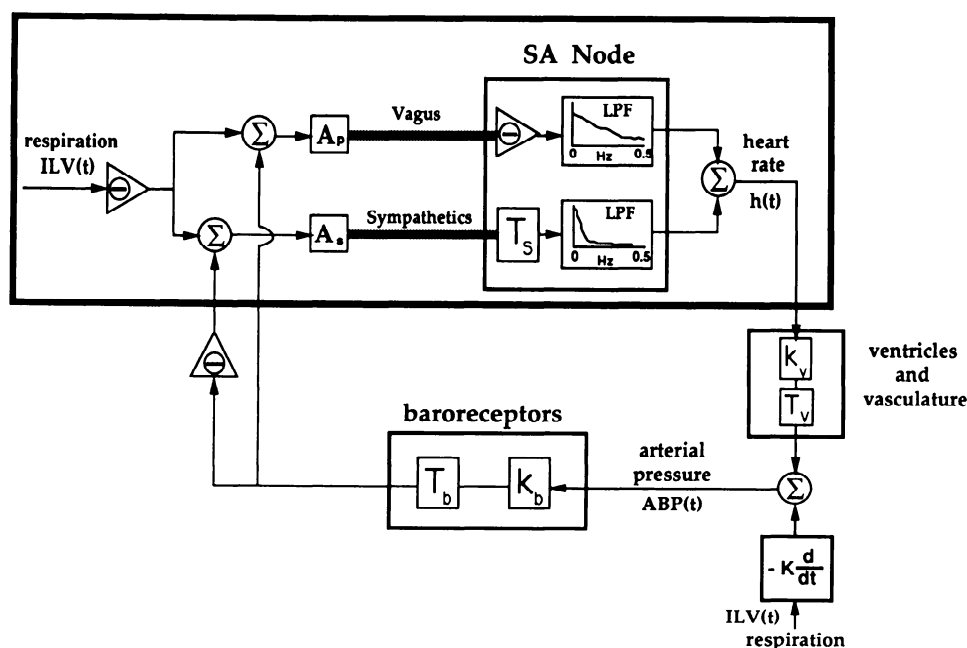

FIG. 9. Simple model of closed-loop cardiovascular regulation proposing that respiration (ILV) affects ABP both by directly inducing HR fluctuations (RSA) and by mechanical coupling to arterial vasculature within the thorax. A model for the RSA component was proposed previously and is enclosed by heavy black box (9). Mechanical component expresses itself as derivative of instantaneous lung volume. Model components are described in detail in APPENDIX A. LPF, low-pass filter.

The low-pass filters, H_p and H_s, were implemented as the complex functions

$$H_p(f) = \frac{K_p f_p}{f_p + jf} \qquad (A2)$$

$$H_s(f) = \frac{K_s f_s}{f_s + jf} \qquad (A3)$$

where K_p and K_s are gain factors and f_p and f_s represent the corner frequencies for the SA nodal response to parasympathetic and sympathetic fluctuations, respectively. Given a certain mean level of vagal and sympathetic activity, these parameters are obtained from the transfer functions shown in Figs. 5A and 6A of Ref. 11. The gain factor equals the Y-intercept of the corresponding transfer magnitude curve, and the corner frequency is the point where the magnitude has fallen 3 dB (a factor of 0.707) from its value at DC. The delay element is implemented using Eq. A1.

Because the transfer relation for each block of the model can be expressed as an explicit function of frequency f, the transfer functions noted above can all be solved in closed form. Given choices for the model parameters, the transfer functions can then be plotted as a function of frequency. Table 2 defines the various model parameters used to model the five physiological states investigated: supine position-control, standing position-control, pure vagal, pure sympathetic, and combined blockade.

The model results for the ILV-HR transfer relations (Fig. 4) were remarkably similar to the experimental results for all the experimental conditions: pure vagal, pure sympathetic, and the

TABLE 2. Model parameters

	Supine	Upright	Vagal	Sympathetic	Combined Blockade
A_p, Hz/l	2.5	1.6	2.5	0.1	0.1
A_s, Hz/l	0.4	2.0	0.1	4.0	0.1
f_p mean, Hz	4	1	4	1	1
f_p corner, Hz	0.2	0.07	0.2	0.07	0.07
K_p, beats·min^{-1}·Hz^{-1}	6	11	6	1	1
f_s mean, Hz	1.0	1.0	0.5	1.25	0.5
f_s corner, Hz	0.015	0.015	0.015	0.015	0.015
K_s, beats·min^{-1}·Hz^{-1}	18	1	1	9	1

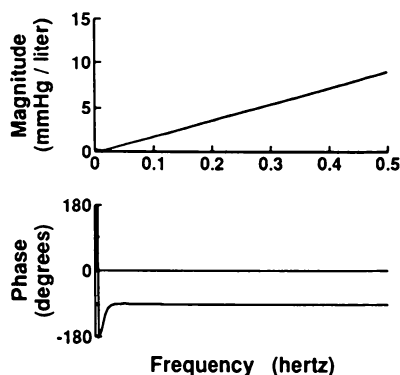See model description in APPENDIX A for definition of variables.

FIG. 10. Model result for transfer relation between ILV and ABP after combined autonomic blockade can be compared to the ILV-PP transfer relations in Fig. 6. Magnitude and phase characteristics are those of a negative derivative. Because parasympathetic and sympathetic gain factors were not set to 0 (Table 2), model changes its characteristics at very low frequencies where gain of a derivative approaches 0.

mixed states of supine and standing control without autonomic blockade. The important similar features one should note are that for both the experimental and model results 1) the transfer relation in both the vagal and sympathetic states can be characterized as a low-pass filter, where the vagal filter demonstrates relatively broad-pass magnitude properties with near zero phase at all relevant frequencies, whereas the sympathetic filter shows a marked drop in magnitude with frequency and a phase delay; 2) the vagal phase approaches 0° at DC (0 Hz), whereas the sympathetic phase approaches 180° at DC; and 3) the phase near 0.15 Hz is ~0° for both systems. The physiological implications of these findings are addressed in the DISCUSSION. It should also be noted that the model results for the mixed states of supine and standing (Fig. 4B) were quite similar to the experimental results despite the simplifying assumptions of linearity in this model.

The model and experimental results for the ABP-HR transfer relations (Fig. 8) were not as similar as those for the ILV-HR relations. For the sympathetic state the model results were not very close to the experimental ones, probably reflecting the fact that the model does not include any mechanism by which ABP fluctuations can arise independent of the HR baroreflex, e.g., through control of the peripheral vasculature via the resistance baroreflex. Interestingly, the model predicted a resonance in the ABP-HR relation at ~0.05 Hz. Although this resonance was not observed experimentally, 0.05 Hz is a frequency at which very prominent oscillations are often seen in HR, ABP, and phrenic and sympathetic nerve activity during various types of hemodynamic stress (32, 35, 38).

Remarkably, in the mixed autonomic states of supine and standing, the model results were quite similar to the experimental ones, despite the absence of vascular resistance control via the arterial baroreflex. For both the model and experimental data the phase at frequencies above 0.1 Hz hovers between 0 and 180°, testifying to the fact that neither the experimental nor the model results can be explained using simple notions of the open-loop feedback or feedforward responses between ABP and HR. These findings further support the notion that, for the ABP-HR relation, analysis methods that do not include causality may be incomplete.

Finally, when the mechanical effect of respiration on ABP was modeled as a negative differentiator, the model results for combined blockade (Fig. 10) closely matched the experimental results for ILV-PP (Fig. 6) at frequencies between 0.1 and 0.5 Hz. Because the differentiator was built into the model based on the experimental results, this similarity is not unexpected but it does help demonstrate graphically the behavior of ILV-PP.

The results of our simple linear model do not account for all the observed experimental phenomena, but they do mimic the data closely enough to suggest that, for small fluctuations around the mean operating point, the complex physiological relations between respiration, HR, and arterial pressure can be quantitatively characterized with linear transfer function techniques.

APPENDIX B

Group-Average Estimates and Error Functions

Deviation between any individual transfer function estimate and the "true" group-average transfer function consists of two components. First, there is a measurement variance associated with each individual transfer function computation that results from imperfect coherence. We have shown previously that the measurement variance $\pi_{mag,i}^2(f)$ associated with the ith individ-

ual transfer magnitude estimate is

$$\pi_{\text{mag},i}{}^2(f) = K|H_i(f)|^2 \left[\frac{1 - \gamma_i^2(f)}{\gamma_i^2(f)} \right] \quad (B1)$$

where $H_i(f)$ and $\gamma_i^2(f)$ are the ith individual transfer and squared coherence functions and K is a constant related to the degree of spectral smoothing (11). The measurement variance $\pi_{\text{phase},i}{}^2(f)$ associated with the corresponding phase estimate is

$$\pi_{\text{phase},i}{}^2(f) = \left[\sin^{-1} \left[\frac{\pi_{\text{mag},i}(f)}{|H_i(f)|} \right] \right]^2 \quad (B2)$$

The second component of estimation error is population variance; i.e., even if an individual transfer function had no measurement error, it would be expected to differ from the true group-average transfer function by the standard deviation in the distribution of observations. We denote the population variance in the magnitude estimate as $\rho_{\text{mag}}{}^2(f)$ and in the phase estimate as $\rho_{\text{phase}}{}^2(f)$. Since the measurement and population variances are independent, we calculate the total variance for the ith transfer magnitude estimate, denoted $\sigma_{\text{mag},i}{}^2(f)$, as

$$\sigma_{\text{mag},i}{}^2(f) = \pi_{\text{mag},i}{}^2(f) + \rho_{\text{mag}}{}^2(f) \quad (B3)$$

and the total variance for the ith phase estimate, denoted $\sigma_{\text{phase},i}{}^2(f)$, as

$$\sigma_{\text{phase},i}{}^2(f) = \pi_{\text{phase},i}{}^2(f) + \rho_{\text{phase}}{}^2(f) \quad (B4)$$

These estimator variances are then used as weights in calculating the group-average transfer magnitude estimate $|\hat{H}(f)|$. Thus

$$|\hat{H}(f)| = \frac{\sum_{i=1}^{N} [|H_i(f)|/\sigma_{\text{mag},i}{}^2(f)]}{\sum_{i=1}^{N} [1/\sigma_{\text{mag},i}{}^2(f)]} \quad (B5)$$

where N is the number of individual estimates contributing to the group average. The standard error $\epsilon_{\text{mag}}(f)$ associated with this estimate is then

$$\epsilon_{\text{mag}}(f) = \frac{1}{\left[\sum_{i=1}^{N} 1/\sigma_{\text{mag},i}{}^2(f) \right]^{1/2}} \quad (B6)$$

To estimate the group-average transfer phase at each frequency, we first derive for each individual transfer estimate a unit vector with the same phase angle. Thus the real part $a_i(f)$ and imaginary part $b_i(f)$ of the unit vector corresponding to the ith individual transfer function are

$$a_i(f) = \cos \theta_i(f) \quad (B7)$$

and

$$b_i(f) = \sin \theta_i(f) \quad (B8)$$

The group-average phase estimate $\hat{\theta}(f)$ is then taken as the angle of the weighted vector sum of these unit vectors

$$\hat{\theta}(f) = \tan^{-1} \left[\frac{\sum_{i=1}^{N} b_i(f)/\sigma_{\text{phase},i}{}^2(f)}{\sum_{i=1}^{N} a_i(f)/\sigma_{\text{phase},i}{}^2(f)} \right] \quad (B9)$$

The standard error $\epsilon_{\text{phase}}(f)$ associated with this phase estimate is

$$\epsilon_{\text{phase}}(f) = \frac{1}{\left[\sum_{i=1}^{N} 1/\sigma_{\text{phase},i}{}^2(f) \right]^{1/2}} \quad (B10)$$

REFERENCES

1. AKSELROD, S., D. GORDON, J. B. MADWED, N. C. SNIDMAN, D. C. SHANNON, AND R. J. COHEN. Hemodynamic regulation: investigation by spectral analysis. *Am. J. Physiol.* 249 (*Heart Circ. Physiol.* 18): H867–H875, 1985.
2. ALLISON, J. L., K. SAGAWA, AND M. KUMADA. An open-loop analysis of the aortic arch barostatic reflex. *Am. J. Physiol.* 217: 1576–1584, 1969.
3. ANGELONE, A., AND N. A. COULTER. Respiratory sinus arrhythmia: a frequency dependent phenomenon. *J. Appl. Physiol.* 19: 479–482, 1964.
4. ANREP, G. V., W. PASCUAL, AND R. ROSSLER. Respiratory variations of the heart rate. II. The central mechanism of the respiratory arrhythmia and the inter-relations between the central and reflex mechanisms. *Proc. R. Soc. Lond. B. Biol. Sci.* 119: 218–232, 1936.
5. APPEL, M. L., J. P. SAUL, R. D. BERGER, AND R. J. COHEN. Closed loop identification of cardiovascular regulatory mechanisms. *Comp. Cardiol.* 1989.
6. BAINBRIDGE, F. A. The influence of venous filling upon the rate of the heart. *J. Physiol. Lond.* 50: 65–84, 1915.
7. BAINBRIDGE, F. A. The relation between respiration and the pulse-rate. *J. Physiol. Lond.* 54: 192–202, 1920.
8. BASELLI, G., S. CERUTTI, S. CIVARDI, A. MALLIANI, AND M. PAGANI. Cardiovascular variability signals: towards the identification of a closed-loop model of the neural control mechanisms. *IEEE Trans. Biomed. Eng.* 35: 1033–1046, 1988.
9. BERGER, R. D. *Analysis of the Cardiovascular Control System Using Broad-Band Stimulation.* (PhD thesis). Cambridge MA: MIT, 1987.
10. BERGER, R. D., S. AKSELROD, D. GORDON, AND R. J. COHEN. An efficient algorithm for spectral analysis of heart rate variability. *IEEE Trans. Biomed. Eng.* BME-33: 900–904, 1986.
11. BERGER, R. D., J. P. SAUL, AND R. J. COHEN. Transfer function analysis of autonomic regulation. I. The canine atrial rate response. *Am. J. Physiol.* 256 (*Heart Circ. Physiol.* 25): H142–H152, 1989.
12. BERGER, R. D., J. P. SAUL, AND R. J. COHEN. Assessment of autonomic response by broad-band respiration. *IEEE Trans. Biomed. Eng.* BME-36: 1061–1065, 1989.
13. BERNARDI, L., F. KELLER, M. SANDERS, P. S. REDDY, F. MENO, AND M. R. PINSKY. Respiratory sinus arrhythmia in the denervated human heart. *J. Appl. Physiol.* 67: 1447–1455, 1989.
14. BLINKS, J. R. Positive chronotropic effect of increasing right atrial pressure in the isolated mammalian heart. *Am. J. Physiol.* 186: 299–303, 1956.
15. BORST, C., AND J. K. KAREMAKER. Time delays in the human baroreceptor reflex. *J. Auton. Nerv. Syst.* 9: 399–409, 1983.
16. CLYNES, M. Respiratory sinus arrhythmia: laws derived from computer simulation. *J. Appl. Physiol.* 15: 863–874, 1960.
17. DAVIES, C. T. M., AND J. M. M. NEILSON. Sinus arrhythmia in man at rest. *J. Appl. Physiol.* 22: 947–955, 1967.
18. DEBOER, R. W., J. M. KAREMAKER, AND J. STRACKEE. Hemodynamic fluctuations and baroreflex sensitivity in humans: a beat-to-beat model. *Am. J. Physiol.* 253 (*Heart Circ. Physiol.* 22): H680–H689, 1987.

19. ECKBERG, D. L. Human sinus arrhythmia as an index of vagal cardiac outflow. *J. Appl. Physiol.* 54: 961–966, 1983.
20. ECKBERG, D. L., Y. T. KIFLE, AND V. L. ROBERTS. Phase relationship between normal human respiration and baroreflex responsiveness. *J. Physiol. Lond.* 304: 489–502, 1980.
21. ECKBERG, D. L., C. NERHED, AND B. G. WALLIN. Respiratory modulation of muscle sympathetic and vagal cardiac outflow in man. *J. Physiol. Lond.* 365: 181–196, 1985.
22. FOUAD, F. M., R. C. TARAZI, C. M. FERRARIO, S. FIGHALY, AND C. ALICANDRI. Assessment of parasympathetic control of heart rate by a noninvasive method. *Am. J. Physiol.* 246 (*Heart Circ. Physiol.* 15): H838–H842, 1984.
23. HAYMET, B. T., AND D. I. McCLOSKEY. Baroreceptor and chemoreceptor influences on heart rate during the respiratory cycle in the dog. *J. Physiol. Lond.* 245: 699–712, 1975.
24. HIRSCH, J. A., AND B. BISHOP. Respiratory sinus arrhythmia in humans: how breathing pattern modulates heart rate. *Am. J. Physiol.* 241 (*Heart Circ. Physiol.* 10): H620–H629, 1981.
25. JOSE, A. D., AND R. R. TAYLOR. Autonomic blockade by propranolol and atropine to study intrinsic myocardial function in man. *J. Clin. Invest.* 48: 2019, 1969.
26. JURGEN, P., C. FRASER, R. S. STUART, W. BAUMGARTNER, AND J. L. ROBOTHAM. Negative intrathoracic pressure decreases independently left ventricular filling and emptying. *Am. J. Physiol.* 257 (*Heart Circ. Physiol.* 26): H120–H131, 1989.
27. JURGEN, P., M. K. KINDRED, AND J. L. ROBOTHAM. Transient analysis of cardiopulmonary interactions. I. Diastolic events. *J. Appl. Physiol.* 64: 1506–1517, 1988.
28. JURGEN, P., M. K. KINDRED, AND J. L. ROBOTHAM. Transient analysis of cardiopulmonary interactions. I. Systolic events. *J. Appl. Physiol.* 64: 1518–1526, 1988.
29. KATONA, P. G., AND F. JIH. Respiratory sinus arrhythmia: noninvasive measure of parasympathetic cardiac control. *J. Appl. Physiol.* 39: 801–805, 1975.
30. KATONA, P. G., J. W. POITRAS, G. O. BARNETT, AND B. S. TERRY. Cardiac vagal efferent activity and heart period in the carotid sinus reflex. *Am. J. Physiol.* 218: 1030–1037, 1970.
31. LEVY, M. N., H. DEGEEST, AND H. ZIESKE. Effects of respiratory center activity on the heart. *Circ. Res.* 18: 67–78, 1966.
32. MADWED, J. B., K. E. SANDS, J. P. SAUL, AND R. J. COHEN. Spectral analysis of beat-to-beat variability in heart rate and arterial blood pressure during hemorrhage and aortic constriction. In: *Neural Mechanisms and Cardiovascular Disease*, edited by B. Lown, A. Malliani, and M. Porsdecimi. Padua, Italy: Liviana, 1986, p. 291–302.
33. MELCHER, A. Respiratory sinus arrhythmia in man. A study in heart rate regulating mechanisms. *Acta Physiol. Scand. Suppl.* 435: 1–31, 1976.
34. MELCHER, A. Carotid baroreflex heart rate control during the active and the assisted breathing cycle in man. *Acta Physiol. Scand.* 108: 165–171, 1980.
35. NINOMIYA, I., K. KUJIME, N. NISHIURA, AND K. SADA. In: *Mechanisms of Blood Pressure Waves*, edited by K. Miyakawa, H. P. Koepchen, and C. Polosa. Tokyo: Japan Scientific Soc. Press, 1984, p. 360.
36. OLSEN, C. O., G. S. TYSON, G. W. MAIER, J. W. DAVIS, AND F. S. RANKIN. Diminished stroke volume during inspiration: a reverse thoracic pump. *Circulation* 72: 668–679, 1985.
37. PARATI, G., M. DIRIENZO, G. BERTINIERI, G. POMIDOSSI, R. CASADEI, A. GROPPELLI, A. PEDOTTI, A. ZANCHETTI, AND G. MANCIA. Evaluation of the baroreceptor-heart rate reflex by 24-hour intraarterial blood pressure monitoring in humans. *Hypertension Dallas* 12: 214–222, 1988.
38. PREISS, G., S. ISCOE, AND C. POLOSA. Analysis of a periodic breathing pattern associated with Mayer waves. *Am. J. Physiol.* 228: 768–774, 1975.
39. RAEDER, E. A., R. BERGER, R. KENET, J. P. KIELY, H. LEHNERT, R. J. COHEN, AND B. LOWN. Assessment of autonomic cardiac control by power spectrum of heart rate fluctuations. *J. Appl. Cardiol.* 2: 283–300, 1987.
40. SAUL, J. P., R. D. BERGER, M. H. CHEN, AND R. J. COHEN. Transfer function analysis of autonomic regulation. II. Respiratory sinus arrhythmia. *Am. J. Physiol.* 256 (*Heart Circ. Physiol.* 25): H153–H161, 1989.
41. SCHER, A. M., AND A. C. YOUNG. Reflex control of heart rate in the unanesthetized dog. *Am. J. Physiol.* 218: 780–789, 1970.
42. SMYTH, H. S., P. SLEIGHT, AND G. W. PICKERING. Reflex regulation of arterial pressure during sleep in man. *Circ. Res.* 24: 109–121, 1969.
43. WEST, J. B. *Ventalation*. In: *Respiratory Physiology*. Baltimore, MD: Williams & Wilkins, 1979, chapt. 4, p. 103.